ACS SyntheticBiology

Research Article

pubs.acs.org/synthbio

Characterization and Modeling of Transcriptional Cross-Regulation in *Acinetobacter baylyi* ADP1

Dayi Zhang,[†,+] Yun Zhao,[‡,§,+] Yi He,[∥] Yun Wang,[†] Yiyu Zhao,[†,‡] Yi Zheng,[‡] Xia Wei,[‡] Litong Zhang,[‡] Yuzhen Li,[‡] Tao Jin,[‡] Lin Wu,[∥] Hui Wang,[⊥] Paul A. Davison,[†] Junguang Xu,[‡,§,*] and Wei E. Huang*[,†]

[†]Kroto Research Institute, University of Sheffield, Broad Lane, Sheffield S3 7HQ, U.K.

[‡]BGI-Shenzhen, Shenzhen 518083, P.R. China

[§]Shenzhen Key Laboratory of Environmental Microbial Genomics and Application, Shenzhen 518083, P.R. China

[∥]Beijing Institute of Genomics, Chinese Academy of Sciences, Beijing 100029, China

[⊥]Centre for Ecology and Hydrology, Wallingford, Banson Road, Wallingford OX10 8BB, U.K.

Supporting Information

ABSTRACT: Synthetic biology involves reprogramming and engineering of regulatory genes in innovative ways for the implementation of novel tasks. Transcriptional gene regulation systems induced by small molecules in prokaryotes provide a rich source for logic gates. Cross-regulation, whereby a promoter is activated by different molecules or different promoters are activated by one molecule, can be used to design an OR-gate and achieve cross-talk between gene networks in cells. *Acinetobacter baylyi* ADP1 is naturally transformable, readily editing its chromosomal DNA, which makes it a convenient chassis for synthetic biology. The catabolic genes for salicylate, benzoate, and catechol metabolism are located within a supraoperonic cluster (*-sal-are-ben-cat-*) in the chromosome of *A. baylyi* ADP1, which are separately regulated by LysR-type transcriptional regulators (LTTRs). ADP1-based biosensors were constructed in which *salA*, *benA*, and *catB* were fused with a reporter gene cassette *luxCDABE* under the separate control of SalR, BenM, and CatM regulators. Salicylate, benzoate, catechol, and associated metabolites were found to mediate cross-regulation among *sal*, *ben*, and *cat* operons. A new mathematical model was developed by considering regulator-inducer binding and promoter activation as two separate steps. This model fits the experimental data well and is shown to predict cross-regulation performance.

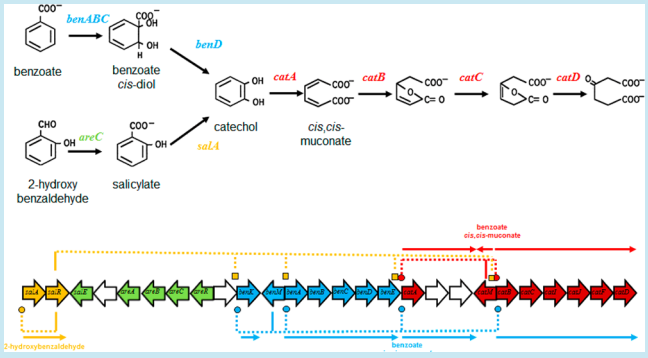

KEYWORDS: *cross-regulation, Acinetobacter baylyi ADP1, catechol, salicylate, benzoate, LysR-type gene regulation, mathematic model, repressor*

One of the important goals of synthetic biology is to reprogram and rewire regulatory genes in innovative ways for the implementation of novel tasks. To help better design a controllable gene network, it is crucial to understand naturally occurring gene regulatory systems and develop mathematic models to predict gene regulation performance. The regulated gene transcription is an essential strategy in prokaryotes for the economic use of energy and enables a rapid response to the changing environment.

The highly naturally transformable bacterium *Acinetobacter baylyi* ADP1 is a convenient chassis for synthetic biology, because its chromosome is readily editable by cutting, deleting, duplicating, and inserting DNA.[1−7] One quarter of the *A. baylyi* ADP1 genome is composed of five major "islands of catabolic pathways".[1] LysR-type transcriptional regulators (LTTRs) control the largest family of transcriptional gene regulation system in prokaryotes.[8] The salicylate, benzoate, and catechol degradation pathways are located in the supercluster *sal-are-ben-cat* in the chromosome of *A. baylyi* ADP1, which are controlled by LysR-type transcriptional regulators SalR, BenM, and CatM separately.[9−12] The *salAR* is controlled by SalR, which can be activated by salicylate.[10] The *benABCDE* operon is regulated by BenM, responding to both benzoate and its metabolite *cis,cis*-muconate.[13] CatM controls transcription of *catA* and the *catBCIJFD* operon and is specifically activated by *cis,cis*-muconate.[14] BenM and CatM are 59% identical in DNA sequence, and both respond to *cis,cis*-muconate to activate transcription.[12] It was previously found that CatM was not involved in *benA* expression.[15] The upstream metabolic pathway of catechol is shown in Figure 1, together with the

Special Issue: Synthetic Biology: Research Perspectives from China

Received: April 1, 2012
Published: June 11, 2012

ACS Publications © 2012 American Chemical Society

dx.doi.org/10.1021/sb3000244 | *ACS Synth. Biol.* 2012, 1, 274−283

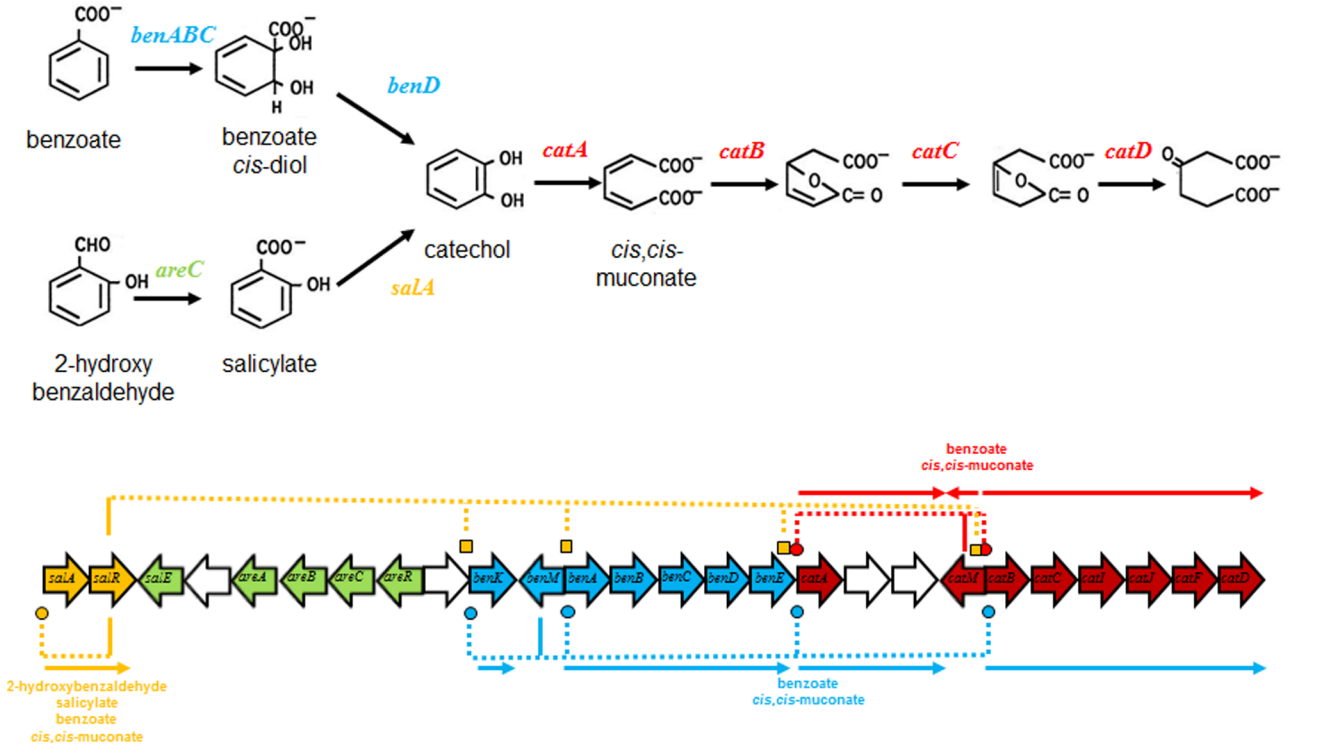

Figure 1. Metabolite pathway and gene structure of supraoperonic cluster *sal-are-ben-cat* in the chromosome of *Acinetobacter baylyi* ADP1. (gold circle) SalR activation promoter. (blue circle) BenM activation promoter. (red circle) CatM activation promoter. (orange box) SalR repression promoter.

Table 1. Strains and Plasmids Used in This Study

strain	description	reference
	Acinetobacter baylyi Strains	
ADP1 (BD413)	Wild type	24
ADPWH_lux	Biosensor of salicylate. A promoterless *luxCDABE* from pSB417 was inserted between *salA* and *salR* genes in the chromosome of ADP1.	3
ADPWH_BenM	Biosensor of benzoate. A promoterless *luxCDABE* from pSB417 was inserted into *benA* gene in the chromosome of ADP1.	this study
ADPWH_CatM	Biosensor of catechol. A promoterless *luxCDABE* from pSB417 was inserted into *catB* gene in the chromosome of ADP1.	this study
ADPWH_ΔSalR	Mutant of ADPWH_lux. A 4-bp deletion was made in the chemical binding module of *salR* regulatory gene in ADPWH_lux chromosome.	4
ADPWH_CatM_ΔSalR	Mutant of ADPWH_CatM. A 4-bp deletion was made in the chemical binding module of *salR* regulatory gene in ADPWH_CatM chromosome.	this study
	Escherichia coli Strains	
DH5α	High efficiency competent cells.	
	Plasmid	
pGEM-T	Amp^r, T7 and SP6 promoters, *lacZ*, vector.	
pSB417	*luxCDABE* source plasmid, The *luxCDABE* cassette was originally from *Photorhabdus (Xenorhabdus) luminescens* ATCC2999 (Hb strain).	23
pUTKm1	Source of kanamycin resistance gene.	25
pGEMT_BenMA_EB	*benMA* with *Eco*RI/*Bam*HI (1105 bp) are inserted into pGEM-T.	this study
pGEMT_BenMA_lux	*luxCDABE* (5846 bp) from pSB417 was inserted at *Eco*RI site of pGEMT_BenMA_EB.	this study
pGEMT_BenMA_lux_KM	km^r (1708 bp) from pUTKm1 was inserted at *Bam*HI site of pGEMT_BenMA_lux.	this study
pGEMT_CatMB_E	*catMB* with *Eco*RI (981 bp) was inserted into pGEM-T.	this study
pGEMT_CatMB_lux	*luxCDABE* (5846 bp) from pSB417 was inserted at *Eco*RI site of pGEMT_CatMB_E.	this study
pGEMT_CatMB_lux_KM	km^r (1708 bp) from pUTKm1 was inserted at *Bam*HI site of pGEMT_CatMB_lux.	this study

gene structure of *salAR*, *catBCIJFD*, and *benABCDE* operon on the chromosome of *A. baylyi* ADP1.

Cross-regulation, which refers to either a single promoter that is activated by different molecules or different promoters that are activated by one molecule, is found among the *sal-are-ben-cat* cluster. In this study, SalR was found to be a repressor not only to the *salAR* operon but also to the *catBCIJFD* and *benABCDE* operons that are controlled by CatM and BenM. SalR, BenM, and CatM regulated operons were cross-regulated and activated by small molecules salicylate, benzoate, catechol, or *cis,cis*-muconate but at different transcriptional levels. Traditional mathematic models are not suitable to simulate

dx.doi.org/10.1021/sb3000244 | *ACS Synth. Biol.* 2012, 1, 274–283

Table 2. Primers Used in This Study

primer	sequence (5′-3′)	note
catM-F-out	TCAGGTAACAAACCATACAGTAAGGAG	outside *catM* gene
catM-F	GGGGCGGCTGGGCAATACACAACTT	internal *catM* gene
catB-R	GCACTGTCTGGGCCAGTCAAGACCTCAT	internal *catB* gene
catMB-R	TGATGGACAACAGAATTCGCTTGAAATAGGTG	created *Eco*RI site
catMB-F	CACCTATTTCAAGCGAATTCTGTTGTCCATC	created *Eco*RI site
catB-R-out	TGCCACCATATAGACTGATTCCAGC	outside *catB* gene
benM-F-out	TTGATTAAGCGGATGGCTGGCATATA	outside *benM* gene
benM-R-out	CATCGCGCGAATGGTATCACCTGCCT	outside *benA* gene
benM-F	CCGGCATCGATACGGCCTTCTTTTAATG	internal *benM* gene
benA-R	CATCGCTTGGATCTTTCACCTTCAAC	internal *benA* gene
benMA-R	AGCCAAATAAACGGATCCGAATTCCCAATTTCCTTCGAA AAT	created *Eco*RI and *Bam*HI sites
benMA-F	AATTGGGAATTCGGATCCGTTTATTTGGCT	created *Eco*RI and *Bam*HI sites
luxC-R	GAGAGTCATTCAATATTGGCAGG	internal *luxC* gene
luxE-F	TGGTTTACCAGTAGCGGCACG	internal *luxE* gene
luxE-F_2	CAGTTATCCAGCATTTATTGTTACC	internal *luxE* gene

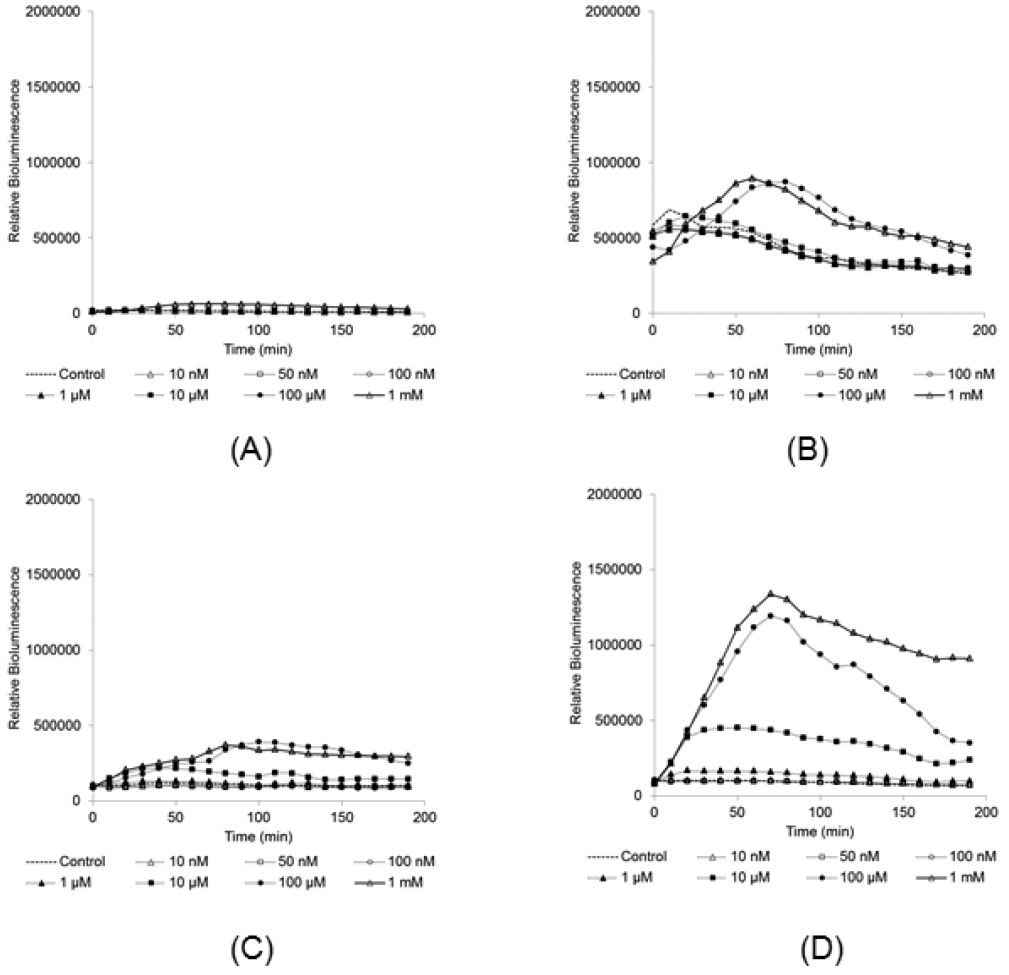

Figure 2. Time course curve of biosensor response to catechol: (A) ADPWH_lux, (B) ADPWH_BenM, (C) ADPWH_CatM, (D) ADPWH_CatM_ΔSalR. The biosensors were induced by catechol from 0 (control) to 1 mM under the same conditions. The baselines of these 4 biosensors were different, and the baseline of ADPWH_BenM was significantly higher than those of the other three biosensors. The response of ADPWH_CatM_ΔSalR to catechol was significantly higher than that of ADPWH_CatM.

cross regulation because they treat regulator-inducer binding and promoter activation as a single step that cannot distinguish between the different regulator-inducer interactions and transcriptional activations. We developed a new mathematical model by considering regulator-inducer binding and promoter activation as two separate steps. The new model fits the experimental results well and has been shown to predict a cross-regulation by applying the same parameters to a new gene regulation system. This model would offer a novel approach to design and optimize the gene regulation network in terms of adjusting the cross-regulation effects.

dx.doi.org/10.1021/sb3000244 | *ACS Synth. Biol.* 2012, 1, 274–283

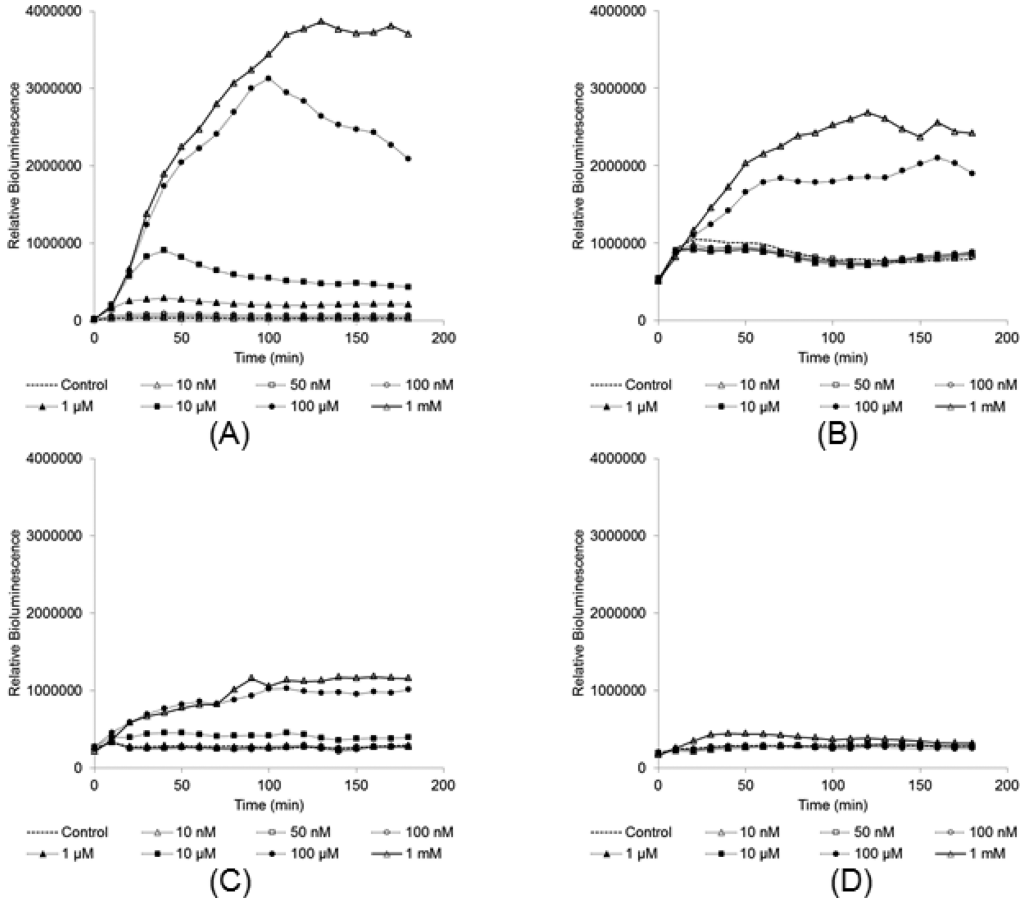

Figure 3. Time course curve of biosensors response to salicylate: (A) ADPWH_lux, (B) ADPWH_BenM, (C) ADPWH_CatM, (D) ADPWH_CatM_Δ*Sal*R. The biosensors were induced by salicylate from 0 (control) to 1 mM under the same conditions. ADPWH_lux showed the most sensitive and strongest response. ADPWH_CatM_Δ*Sal*R was silent to salicylate, indicating CatM cannot recognize salicylate to trigger the *catB* gene expression. The small induction of ADPWH_CatM_Δ*Sal*R when exposed to high concentrations of salicylate was due to leakage of *salA* expression, which converted salicylate into the inducer *cis*,*cis*-muconate.

RESULTS AND DISCUSSION

Gene Structure of BenM and CatM Regulated Biosensors. ADPWH_BenM was constructed by inserting a promoterless *luxCDABE* cassette into the *benA* gene in the ADP1 chromosome, which is controlled by the BenM regulator.[12] PCR and DNA sequencing results using the primer pair benM-F-out/luxC-rev (Table 2) confirmed the location of *luxCDABE* on the chromosome of ADPWH_BenM. Since wild type *A. baylyi* ADP1 cannot grow in 300 μg/mL ampicillin within 24 h, the positive growth of ADPWH_BenM under this condition indicated that it contains an ampicillin-resistant gene. It suggests that the whole plasmid pBenMA_lux_KM (containing the Amp^r gene) has been integrated into the chromosome of ADPWH_BenM via Campbell-type recombination (Supplementary Figure S1A). The metabolic pathway from benzoate to *cis*,*cis*-muconate is still intact in ADPWH_BenM (Figure 1).

The *catB* is regulated by the LysR-type CatM (Figure 1).[12] ADPWH_CatM and ADPWH_CatM_Δ*Sal*R have been constructed by inserting a promoterless *luxCDABE* cassette into *catB* gene on the chromosome of ADP1 and ADPWH_Δ*Sal*R (Table 1, Supplementary Figure S1). The insertions in the chromosome in ADPWH_CatM and ADPWH_CatM_Δ*Sal*R were confirmed by PCR and DNA sequencing using the two primer pairs catM-F-out/luxC-rev and catB-R-out/luxE-F_2 (Table 2) (Supplementary Figure S1B). In addition, both ADPWH_CatM and ADPWH_CatM_Δ*Sal*R cannot grow on LB agar supplemented with 300 μg/mL ampicillin, suggesting the insertion has occurred via homologous recombination (Supplementary Figure S1B).

Biosensors Induced by Catechol. Three biosensors containing intact *salR*, namely, ADPWH_CatM, ADPWH_lux, and ADPWH_BenM, show moderate responses to catechol (Figure 2) with the maximum response ratio of 3.84, 7.54, and 3.13 respectively in the presence of 1 mM catechol. In contrast, ADPWH_CatM_Δ*Sal*R, in which *salR* was disrupted by a 4-bp deletion,[4] was strongly activated by catechol (Figure 2) with a maximum response ratio of 17.46 to 1 mM catechol. It is notable that the only difference between ADPWH_CatM and ADPWH_CatM_Δ*Sal*R is functionality of SalR (Table 1). The strong catechol induction in ADPWH_CatM_Δ*Sal*R (Figure 2) indicates that the functionality of SalR affects CatM regulatory performance. It is likely that SalR and CatM competitively bind the *catB* promoter and that catechol molecules will bind to CatM and trigger the expression of the *catBCIJFD* operon in ADPWH_CatM_Δ*Sal*R where SalR is non-functional (Figure 2). The low baseline of the *salAR* operon expression in ADPWH_lux (Figure 2) suggests that it is tightly repressed by its regulator SalR. Indeed, a previous study on SalR mutation indicated that disruption of the DNA binding domain (DBD) of SalR increased the *sal* operon background expression.[4] These results suggest that SalR, like CatM and

dx.doi.org/10.1021/sb3000244 | *ACS Synth. Biol.* 2012, 1, 274–283

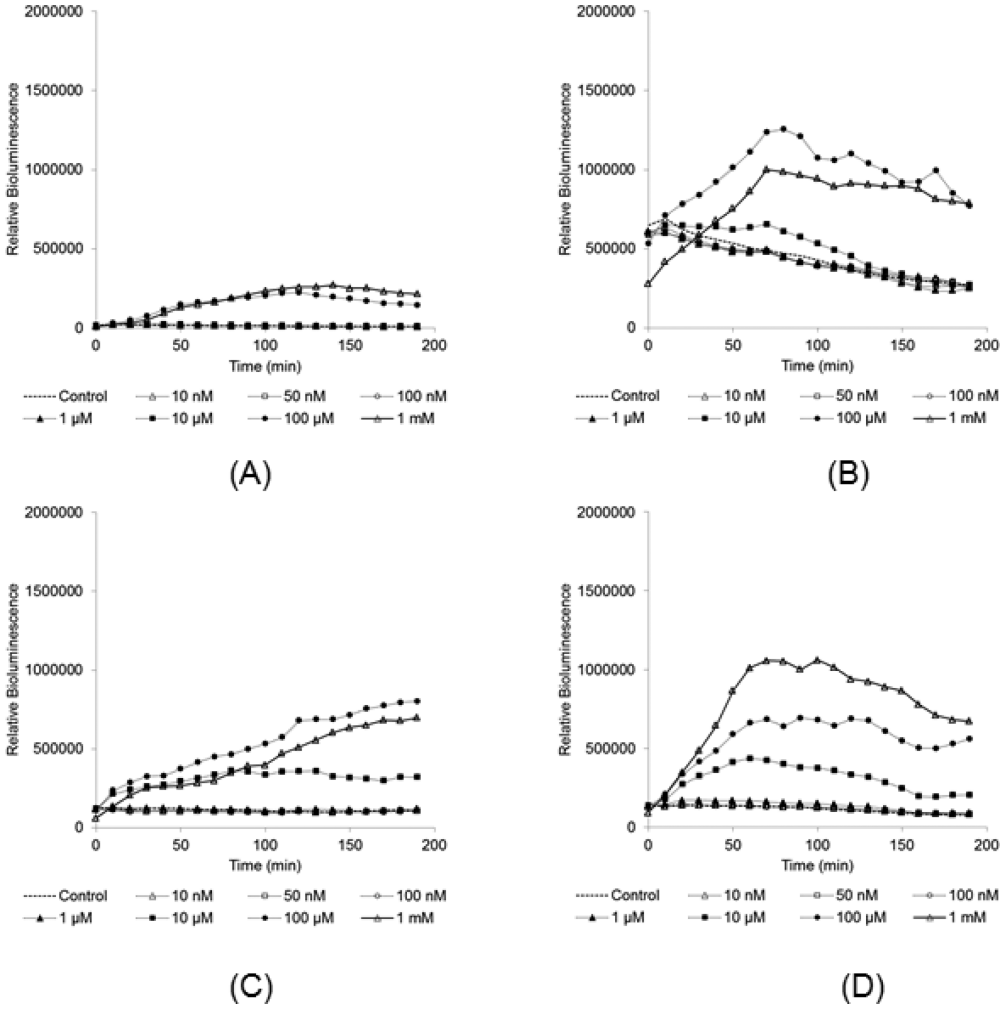

Figure 4. Time course curve of biosensors response to benzoate: (A) ADPWH_lux, (B) ADPWH_BenM, (C) ADPWH_CatM, (D) ADPWH_CatM_ΔSalR. The biosensors were induced by benzoate from 0 (control) to 1 mM under the same conditions.

BenM,[5,9] is also a repressor and that it not only represses the *salAR* operon but also crossly represses the expression of the *catBCIJFD* and *benABCDE* operons (Figure 2). The strong background of ADPWH_BenM (Figure 2), when compared with ADPWH_lux, ADPWH_CatM, and ADPWH_CatM_ΔSalR, indicates that BenM is a relatively weaker repressor than SalR and CatM.

Biosensors Induced by Salicylate. The high response of ADPWH_lux to salicylate indicates that the SalR regulator senses and binds salicylate to activate the *salAR* promoter (Figure 3). Although ADPWH_CatM was responsive to salicylate, ADPWH_CatM_ΔSalR was nearly unresponsive (Figure 3). This suggests that it is salicylate metabolites (likely *cis*,*cis*-muconate as previously suggested[14]), but not salicylate itself, that activates the *catBCIJFD* operon in ADPWH_CatM and the silence of ADPWH_CatM_ΔSalR is due to the nonfunctional *salR* gene that disrupts the salicylate-to- *cis*,*cis*-muconate pathway. A relatively weak induction of ADPWH_CatM_ΔSalR was observed when exposed to high concentrations of salicylate of 0.4−1 mM (Figure 3). It is presumed that a low level leakage of *salA* expression led to a small amount of conversion of salicylate into *cis*,*cis*-muconate that activated a weak expression of the *catBCIJFD* operon. ADPWH_BenM expressed bioluminescence in the presence of salicylate since its pathways from salicylate to muconate were intact (Figure 1). The results in Figure 3 are consistent with previous studies that suggest that a salicylate metabolite, *cis*,*cis*-muconate, is an inducer to BenM and CatM regulators.[9]

Biosensors Induced by Benzoate. ADPWH_lux shows a higher response to benzoate than catechol (Figures 2 and 4), suggesting that benzoate could have a more specific binding capability to the SalR regulator than catechol to trigger *luxCDABE* expression. Previous studies suggested that the response of ADPWH_BenM to benzoate was the result of the interaction between the BenM regulator and both benzoate and *cis*,*cis*-muconate.[5] Since ADPWH_BenM contains an intact benzoate degradation pathway, benzoate can be converted into *cis*,*cis*-muconate (Figure 1), and ADPWH_BenM was thus responsive to benzoate (Figure 4).

Cross Regulation in *Acinetobacter baylyi* ADP1. ADPWH_ΔSalR does not express any bioluminescence in response to salicylate, benzoate, or catechol, indicating the *salAR* operon is silenced due to disruption of the *salR* regulator gene (data not shown). As described before, the SalR regulator could compete with the CatM and BenM to suppress the expression of the *catBCIJFD* operon. Therefore, the disruption of *salR* in the ADPWH_CatM_ΔSalR strain changes the regulator activation probability of CatM or BenM to their promoters, leading to higher gene expression rates to benzoate (9.4) and catechol (16.5) compared with those of ADPWH_-

dx.doi.org/10.1021/sb3000244 | *ACS Synth. Biol.* 2012, 1, 274−283

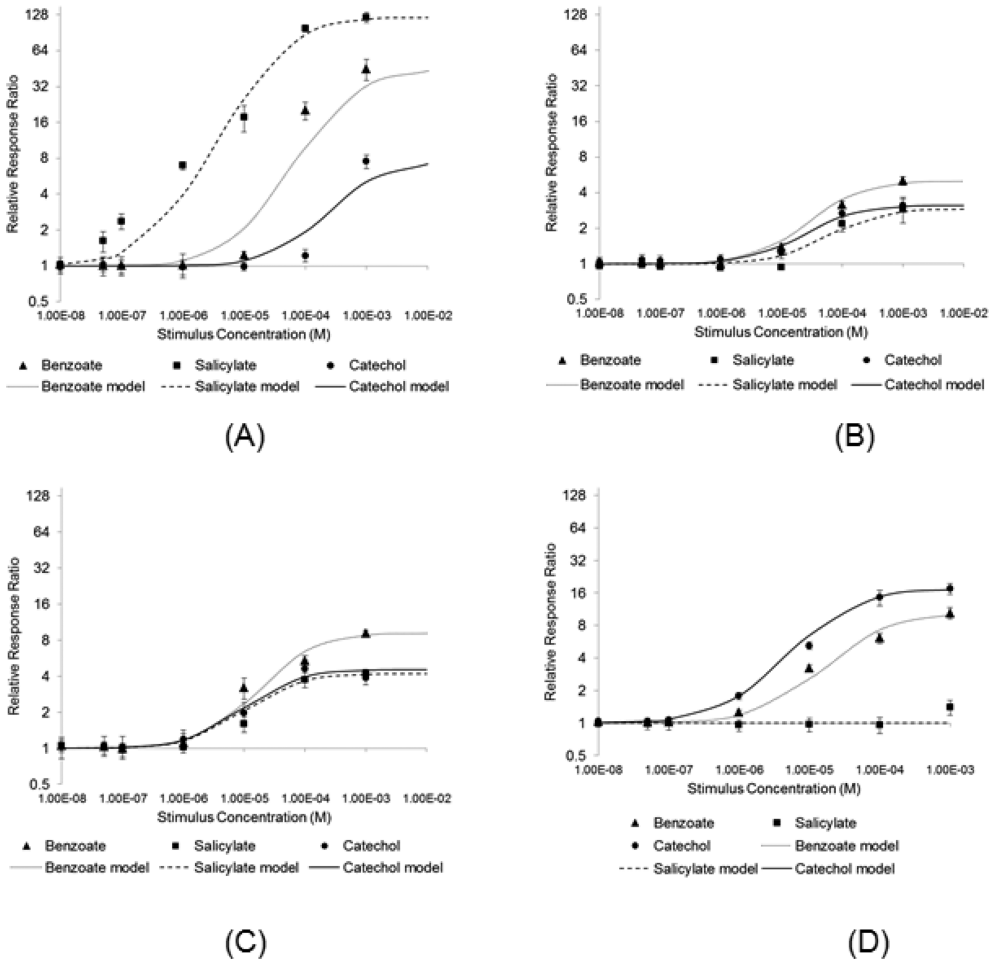

Figure 5. Match of experimental data and model predictions of relative response ratio at different inducer concentrations. (A) ADPWH_lux. (B) ADPWH_BenM. (C) ADPWH_CatM. (D) ADPWH_CatM_ΔSalR. Dots are experimental data obtained from individual biosensor response to inducers. Lines represent the model simulation, the parameters are derived from the new regulation model, and predicted rates of gene expression and specific inducer binding rates are shown in Table 3.

Table 3. Biosensor Respective Response Ratio to Different Inducers

		gene expression rate (s^{-1}·$cell^{-1}$)			special inducer binding rate K_1		
		benzoate	salicylate	catechol	benzoate	salicylate	catechol
experiment	ADPWH_lux	43.9	120.8	6.5	2632	25641	1754
	ADPWH_BenM	4.0	1.9	2.1	17241	9804	24390
	ADPWH_CatM	8.2	3.2	3.5	19231	47619	46948
	ADPWH_CatM_ΔSalR	9.4	0.1	16.5	19608	0	48544
model	ADPWH_CatM_ΔSalR	8.2	0.0	3.5	19231	0	46948

CatM (8.2 and 3.5, respectively), as shown by the results in Figure 5 and Table 3. Lack of competitive binding of SalR, caused the responsive sensitivity of ADPWH_CatM_ΔSalR to catechol to be significantly enhanced, and it was able to detect catechol as low as 0.1 μM in comparison with a 2 μM responsive threshold in ADPWH_CatM (Figure 2). In summary, SalR is a repressor of the *salAR*, *catBCIJFD*, and *benABCDE* operons in the absence of inducer. The SalR regulator can sense both salicylate and benzoate leading to *salA* activation, while the inducer of BenM is benzoate or *cis*,*cis*-muconate. The *catBCIJFD* is regulated by CatM, which recognizes benzoate and *cis*,*cis*-muconate, and its transcription level can be enhanced by deletion of the *salR*. Silencing of the salicylate degradation pathway increases sensitivity of the *catBCIJFD* response to catechol.

Traditional Gene Transcription and Translation Model. *A. baylyi* ADP1 is a well-established model strain for metabolism research due to its genetics and physiological properties.[16] Gene regulation has been modeled to reveal the biochemical and biophysical relationship between gene expression and metabolite pathways. In a classical theoretical analysis, a conventional chemical reaction equation is usually used to describe the processes of transcription and translation[17] as shown in eqs 1−4.

$$\frac{\mathrm{d}[\mathrm{mRNA}]}{\mathrm{d}t} = \alpha_{\mathrm{m,s}} - \gamma_{\mathrm{m}}\cdot[\mathrm{mRNA}] \quad (1)$$

$$[\mathrm{mRNA}]_{\mathrm{stable}} = \alpha_{\mathrm{m}}/\gamma_{\mathrm{m}} \quad (2)$$

dx.doi.org/10.1021/sb3000244 | *ACS Synth. Biol.* 2012, 1, 274−283

$$\frac{d[\text{protein}]}{dt} = \alpha_p \cdot [\text{mRNA}] - \gamma_p \cdot [\text{protein}] \quad (3)$$

$$[\text{protein}]_{\text{stable}} = \frac{\alpha_p \cdot [\text{mRNA}]}{\gamma_p} = \alpha_{m,s} \cdot \frac{\alpha_p}{\gamma_p \cdot \gamma_m} \quad (4)$$

α_m and γ_m represent mRNA synthesis and decay coefficient ($s^{-1}\cdot cell^{-1}$), and α_p and γ_p are protein synthesis and decay coefficient ($s^{-1}\cdot cell^{-1}$). However, in this model mRNA synthesis and translation are assumed to be stable processes, and the promoter activation and inducer binding has been regarded as a single step.[18] Such a simplified assumption cannot explain the stochastic gene expression (noise) that was observed at the single cell level.[19]

To address the problem of intrinsic and extrinsic noise in gene expression, knowing the mRNA synthesis rate is the key factor, but it is still a challenge to measure it. Normally, mRNA synthesis is defined by the classic Hill's gene regulation model as shown in eq 5.

$$\alpha_{[s]} = \alpha \cdot \frac{[S]}{\frac{k^+}{k^-} + [S]} \quad (5)$$

Here α ($s^{-1}\cdot cell^{-1}$) represents the saturated transcription rate when a regulator combines with an inducer, and k^+ and k^- are the chemical reaction rates of the equilibrium ($s^{-1}\cdot cell^{-1}$). When the number of inducers in the cytoplasm is [S] ($cell^{-1}$), the real transcription rate is $\alpha_{[s]}$ ($s^{-1}\cdot cell^{-1}$).

New Mathematical Gene Regulation Model Developed in This Study. Usually inducer-bound regulator is not consumed, which is an assumption made in Hill's equation.[20] The inducer-bound regulator does not help RNA transcription until it is bound to the promoter. It is the dynamic equilibrium between inducer-bound regulator and free regulator that determines the probability of RNA transcription. Such dynamic equilibrium reaches a stable state when inducer concentration is constant.

Here we consider that the extrinsic noise comes from variation in the cellular components of the transcriptional process, such as limitations in the amount of regulatory protein and the different chemical reaction rates of the regulatory protein-inducer interaction and promoter activation of transcription.[21] The new LysR-type gene regulation model is therefore developed in eqs 6−10.

$$[S] + [R] \leftarrow \frac{k_1}{k_1^{-1}} \rightarrow [RS] \xrightarrow{k_m} \text{gene expression} \quad (6)$$

$$[RS] + [R] = [R]_{\text{total}} \quad (7)$$

$$\frac{d[RS]}{dt} = k_1 \cdot [S] \cdot [R] - k_1^{-1}[RS] \quad (8)$$

$$[RS] = [R]_{\text{total}} \cdot \frac{[S]}{\frac{k_1^{-1}}{k_1} + [S]} \quad (9)$$

$$\alpha_{m,s} = (k_m \cdot [R]_{\text{total}}) \cdot \frac{[S]}{K_1^{-1} + [S]} = \alpha_m \cdot \frac{[S]}{K_1^{-1} + [S]} \quad (10)$$

where $[R]_{\text{total}}$ ($cell^{-1}$) represents the total number of the limited regulatory protein, while [RS] ($cell^{-1}$) and [R] ($cell^{-1}$) refer to the proteins combined with inducers and free regulatory protein, respectively. k_1 and k_1^{-1} ($s^{-1}\cdot cell^{-1}$) are the inducer binding and disassociating rates of the equilibrium. k_m ($s^{-1}\cdot cell^{-1}$) is the transcription rate when the operon is triggered by RS, and K_1 is the special inducer binding rate (non-dimensional ratio between k_1 and k_1^{-1}). $\alpha_{m,s}$ ($s^{-1}\cdot cell^{-1}$) and α_m ($s^{-1}\cdot cell^{-1}$) are the transcription rate under [S] and saturated inducer conditions, respectively. From eq 10, the new model follows a similar shape as Hill's equation but assumes two separate steps: the inducer-regulator interaction and promoter activation.

From the Hill's equation, however low the concentration of a substrate is, an induced gene expression would occur; in other words, there is no induction limit and no baseline. However, this simplified model does not fit experimental observations in reality. It is observed that gene expression usually has a non-zero baseline and an inducer-regulated transcription occurs when an inducer's concentration is greater than a threshold. The baselines vary in different gene regulation systems. For example baselines of the *catBCIJFD* and *benABCDE* operons are 100−1000 times stronger than that of the *salAR* operon (Figures 3, 4, and 5). In the new model, an expression background is introduced when inducer concentration is lower than a threshold, and it is shown in eq 11. Here $\alpha_m \cdot ([S])/(K_1^{-1} + [S])$ ($s^{-1}\cdot cell^{-1}$) is the gene expression rate when inducer concentration is [S].

$$\alpha_{[S]} = \alpha_{m[0]} + \alpha_m \cdot \frac{[S]}{K_1^{-1} + [S]} \quad (11)$$

where $\alpha_{m[0]}$ ($s^{-1}\cdot cell^{-1}$) represents the baseline transcription rate when the cells are not exposed to the inducer (based on experimental data). Based on the experimental data obtained in this study, the respective gene expression rate ($k_m \cdot [R]_{\text{total}}$) and special inducer binding rate (K_1) of ADPWH_CatM, ADPWH_BenM, and ADPWH_lux were calculated and are shown in Table 3. By using the same parameters obtained from the simulations of these three biosensors, the predicted performance of ADPWH_CatM_ΔSalR fits the experimental data well (Figure 5D). The correlation coefficients and *p*-values of the model simulation and prediction are shown in Supplementary Table S1, indicating experimental data and the model calculation matched well. It suggests that the new model is valid to simulate this LysR-type of inducer-regulated gene expression. Compared with the classical gene regulation model, the key point of this new model is to separate the two steps of the inducer-regulator interaction and promoter activation. This separation enables the new model to consider the effect of noise and suggests that the baseline is due to stochastic gene expression.

Theoretical and Mathematical Analysis of Cross Gene Regulation. On the basis of these parameters, the behavior of several different biosensors can be simulated when exposed to different concentration of inducers, as shown in Figure 5. From the results of model simulation, ADPWH_lux shows a positive response to all the inducers, but the response ratio varies within a large range. The inducer binding rates indicate that SalR can sense salicylate with high specificity while its recognition of benzoate and catechol is weak. However, the gene expression of benzoate to ADPWH_lux is high, suggesting that SalR-benzoate complex can also effectively activate *salAR*.

As for ADPWH_BenM, its special binding rate K_1 to catechol (24390) is higher than that to benzoate (17241) (Table 3), whereas the gene expression rate to catechol (2.1 $s^{-1}\cdot cell^{-1}$) is lower than that to benzoate (4.0 $s^{-1}\cdot cell^{-1}$). It is

dx.doi.org/10.1021/sb3000244 | ACS Synth. Biol. 2012, 1, 274−283

suggested that the *benABCDE* is activated by *cis*,*cis*-muconate, a metabolite of catechol degradation, and that BenM regulator has more specificity to sense *cis*,*cis*-muconate than benzoate.[12] These results hint that the BenM-benzoate complex has a higher activation capability to trigger gene expression than BenM-*cis*,*cis*-muconate. The inducer binding rate of ADPWH_BenM to salicylate (9804) is much lower than that to catechol (24390), suggesting that salicylate can strongly suppress the *benA* gene expression. Since catechol is a metabolite of salicylate degradation and can be sensed by BenM with high specificity, salicylate must have the capability to bind BenM with a lower gene expression rate.

The special inducer binding rates of ADPWH_CatM to catechol and to benzoate are 46948 and 19231, respectively (Table 3). It suggests that CatM has a high specificity to sense *cis*,*cis*-muconate but a low capability to bind benzoate, resulting in a low binding rate when exposed to benzoate. Since benzoate can be converted into catechol through the metabolite pathway, the binding rate of ADPWH_CatM to benzoate is the combined effects of both catechol and benzoate. Thus, the low binding rates to benzoate suggest that CatM has a high specificity to sense catechol but a low capability to bind benzoate, resulting in low binding rate when exposed to benzoate. On the other hand, the gene expression rate of ADPWH_CatM to benzoate ($8.2\ s^{-1}\cdot cell^{-1}$) is much higher than that to catechol ($3.5\ s^{-1}\cdot cell^{-1}$). Since the *benM* and *catM* both have at least 16 amino acids for aromatic compound sensing and share 59% sequence identity, the regulators BenM and CatM have a similar capability to activate transcription at different locations with homoioplastic response type for benzoate and catechol.[15] The similar special inducer binding rate and gene expression rate of ADPWH_CatM to salicylate and catechol (Table 3) suggest that CatM cannot sense salicylate and the *catBCIJFD* operon expression by salicylate is activated by its metabolite, catechol.

Application of New Model To Predict Performance of ADPWH_CatM_ΔSalR. From the gene expression rate and inducer binding rate analysis, the behavior of ADPWH_CatM_ΔSalR can be predicted on the basis of parameters obtained from the other three biosensors' simulations. On comparison of ADPWH_CatM_ΔSalR and ADPWH_CatM, the only difference is that the salicylate to catechol metabolite pathway is blocked in ADPWH_CatM_ΔSalR due to the disruption of SalR. Because the salicylate path is blocked and salicylate cannot be converted into catechol, ADPWH_CatM_ΔSalR should be silent when salicylate is added. The disruption of SalR does not affect the benzoate or catechol pathway. Thus, ADPWH_CatM_ΔSalR should show a similar response as the ADPWH_CatM when exposed to benzoate or catechol. However, the cross-regulation impacts are considered in the new mathematical model, where the disruption of the *salR* gene can significantly affect the gene expression rates of the *cat* operon due to the suppression of the SalR regulator, but showing no impact on the special inducer binding rate. Indeed, the experimental data show that ADPWH_CatM_ΔSalR has a similar special inducer binding rate as ADPWH_CatM in response to catechol and benzoate while the gene expression rates are different (Table 3). Since benzoate can be converted into catechol through the metabolite pathway, the binding rate of ADPWH_CatM and ADPWH_CatM_ΔSalR to benzoate is due to the combined effects of both catechol and benzoate. The model prediction matches well with the experimental data (Table 3).

Because of the disruption of the *salR* gene, ADPWH_CatM_ΔSalR showed no response to salicylate. The *salA* gene is located upstream of the salicylate metabolic pathway and is not involved in the benzoate and catechol degradation process. Thus, the cross regulation is mainly caused by the SalR regulator. The optimization of catechol upstream can therefore be carried out through two potential approaches, internal regulator evolution and external cross regulation adjustment. The former can be achieved by promoter mutation and direct evolution of regulator protein. The latter, the adjustment of cross regulation, can be achieved by mutating regulatory proteins such as disruption of the SalR repressor in this study. Since our new mathematic model can distinguish regulator-inducer interaction and promoter activation as two separate steps, it would help in the better design of gene networks. Supplementary Figure S2 makes a theoretical prediction of gene expression strength of the *benABCDE* in ADPWH_ΔSalR. The gene expression level of *benA* and *catB* operon changed due to the disruption of the regulator *salR*. It implies that a cross regulation can be adjusted by mutating regulators according to the new model prediction, which would offer a new approach for metabolic pathway reconstruction in synthetic biology.

MATERIALS AND METHODS

Bacteria Strains, Plasmids, Culture Media, and Chemicals. The bacterial strains and plasmids used in this study are listed in Table 1. Luria–Bertani broth (LB) and agar (LBA) (Fisher Scientific) or a minimal medium (MM) were used for bacterial cultivation. One liter of MM contains 2.5 g Na_2HPO_4, 2.5 g KH_2PO_4, 1.0 g NH_4Cl, 0.1 g $MgSO_4{\cdot}7H_2O$, 10 μL $CaCl_2$ solution (745 g/L), 10 μL $FeSO_4$ solution (256 g/L), and 1 mL Bauchop & Elsden solution.[22] MM-succinate (MMS) was prepared by adding 20 mM succinate (final concentration) to MM. A final concentration of 300 μg/mL ampicillin (Amp) or 10 μg/mL kanamycin (Km) for *A. baylyi* ADP1 and its mutants was applied when required. *A. baylyi* strains were grown at 30 °C. All chemicals were purchased from Sigma-Aldrich Co., U.K. and were of analytical grade unless otherwise stated. All of the stock solutions were filter-sterilized by passing through 0.22 μm syringe filters (Millipore Inc.).

Biosensor Construction. To investigate the behavior of the catechol upstream metabolite pathway in *Acinetobacter baylyi* ADP1, five biosensor strains, including ADPWH_lux, ADPWH_CatM, ADPWH_BenM, ADPWH_CatM_ΔSalR, and ADPWH_ΔSalR (Table 1), were characterized in this study. ADPWH_lux was constructed previously with a promoterless *luxCDABE* inserted between *salA and salR* in the chromosome of *Acinetobacter baylyi* ADP1 by homologous recombination.[3] ADPWH_ΔSalR was generated by disrupting the *salR* gene through a 4-bp deletion.[4]

Strain ADPWH_BenM was constructed following the scheme in Supplementary Figure S1A. PCR was used to create *Eco*RI and *Bam*HI sites inside *benA* gene, using the primer pairs benM-F/benMA-R and benA-R/benMA-F and a colony of ADP1 as DNA template (Supplementary Figure S1A and Table 2). Subsequently, *benMA* gene with *Eco*RI and *Bam*HI sites was generated through overlap extension PCR[3,6] with the primer pairs benM-F/benA-R (Supplementary Figure S1A and Table 2). Plasmid pGEMT_BenMA_EB containing fragments of the *benMA* gene with *Eco*RI and *Bam*HI sites was cloned into pGEM-T (Promega, UK) as shown in Supplementary Figure S1, which belongs to a family of cloning vectors that have been

shown not to replicate in ADP1.[2] A promoterless *luxCDABE* from pSB417[23] was then cloned into *Eco*RI site of pGEMT_BenMA_EB to construct pGEMT_BenMA_lux, selected by positive bioluminescence signal on the agar plate (Supplementary Figure S1A). Plasmid pGEMT_BenMA_lux_KM was generated by cloning kanamycin resistant km^r cassette from pUTKm1 into pGEMT_BenMA_lux in *E. coli* DH5α with 100 μg/mL kanamycin as natural selection pressure (Supplementary Figure S1A). Recombination of pGEMT_BenMA_lux_KM with *A. baylyi* ADP1 wild type results in the replacement of *ben*MA fragments, and the transformants were identified on the basis of their ability to grow under 10 μg/mL kanamycin, as shown in Supplementary Figure S1A.

The construction of ADPWH_CatM and ADPWH_CatM_ΔSalR, which are derived from the same plasmid pGEMT_CatMB_lux_KM, followed the scheme in Supplementary Figure S1B. An *Eco*RI site was created by PCR in the *catB* gene using the primer pairs catM-F/catMB-R and catB-R/catMB-F (Supplementary Figure S1B and Table 2), and the *catMB* gene with *Eco*RI site was generated through overlap extension PCR using the primer pairs catM-F/catB-R (Supplementary Figure S1B and Table 2). Plasmid pGEM-T was also used to generate plasmid pGEMT_CatMB_E containing *catMB* cassette with *Eco*RI. A promoterless *luxCDABE* was then cloned into the *Eco*RI site of pGEMT_CatMB_E to construct pGEMT_CatMB_lux, selected by positive bioluminescence signal (Supplementary Figure S1B). Plasmid pGEMT_CatMB_lux_KM was generated as mentioned above by cloning km^r cassette into pGEMT_CatMB_lux (Supplementary Figure S1B). With pGEMT_CatMB_lux_KM as a donor and *A. baylyi* ADP1 wild type or the ADPWH_ΔSalR as recipient, respectively, the *luxCDABE-Km* cassette was inserted into the chromosome through homologous recombination (Supplementary Figure S1B), where the transformants were selected on Luria–Bertani (LB) agar with 10 μg/mL kanamycin.

To confirm the integration of *luxCDABE* into the chromosome, PCR was performed using two primers pairs benM-F-out/luxC-rev and benA-R-out/luxE-F for ADPWH_BenM, and CatM-F-out/luxC-rev and catB-R-out/luxE-F_2 for ADPWH_CatM and ADPWH_CatM_ΔSalR (Figure S1B and Table 2). Here, the benM-F-out and benA-R-out were excluded in the vector pGEMT_BenMA_lux_KM and CatM-F-out and catB-R-out were excluded in the vector pGEMT_CatMB_lux_KM. The PCR products were purified, cloned into pGEM-T vector, and sequenced. All the strains and plasmids used during the construction process are listed in Table1.

Cell Culture and Induction. After growing in LB medium at 30 °C overnight, *Acinetobacter* biosensor cells (10^8 CFU/mL) including ADPWH_CatM, ADPWH_lux, ADPWH_BenM, and ADPWH_CatM_ΔSalR) were harvested by centrifugation at 3000 rpm for 10 min at 4 °C. The cell pellets were subsequently washed and resuspended in deionized water of the same volume. One milliliter of such biosensors was then transferred into 9 mL MMS solution to give biosensor stock solution.

Different inducers, including catechol (1.10 g), sodium benzoate (1.44 g), and sodium salicylate (1.60 g), were each dissolved in 10.0 mL deionized water to give stock solutions with 1.0 M final concentration. The stock solutions were subsequently diluted to give a series of final concentrations of 100 nM, 200 nM, 500 nM, 1 μM, 2 μM, 5 μM, 10 μM, 20 μM, 50 μM, 100 μM, 200 μM, 500 μM, 1 mM, and 10 mM with deionized water. A 180 μL portion of biosensor stock solutions and 20 μL of inducer solutions were added into each well of a black clear-bottom 96-well microplate (Corning Costa, USA). Three replicates were carried out for each sample, and deionized water was used as negative control of inducer.

Bioluminescence Detection and Data Analysis. The microplate was incubated at 30 °C and continuously monitored for 200 min within a Synergy 2 Multimode Microplate Reader (BioTek Instruments, Inc., USA) equipped with Gen5 analysis software. The bioluminescence and OD_{600} were measured every 10 min. Before each measurement, 30 s of vertical shaking was used for better cell suspension. Induced bioluminescence of biosensors was obtained by averaging five monitored bioluminescence data. Bioluminescence response ratio was calculated by dividing induced bioluminescence by original bioluminescence (time = 0). Relevant bioluminescence response ratio was evaluated by dividing induced bioluminescence by bioluminescence of negative control (non-induced) samples.

■ ASSOCIATED CONTENT

Ⓢ Supporting Information

This material is available free of charge via the Internet at http://pubs.acs.org.

■ AUTHOR INFORMATION

Corresponding Author

*E-mail: xujunguang@genomics.org.cn; w.huang@shef.ac.uk.

Author Contributions

[+]These authors contributed equally to this work.

Author Contributions

W.E.H., J.X., H.W., and L.W. designed the experiments. D.Z., Y.Z., Y.H., Y.W., Y.Z., Y.L., T.J., and J.X. performed the biosensor construction. D.Z., Y.W., and Y.Z. performed the biosensor characterization. D.Z. and Y.Z. performed the model simulation. D.Z. and W.E.H. analyzed the data. D.Z. and W.E.H. wrote the manuscript.

Notes

The authors declare no competing financial interest.

■ ACKNOWLEDGMENTS

The work is supported by EPSRC grant EP/H049479/1, Royal Society research fund and EU grant ECOWATER (RFCR-CT-2010-00010) to W. E. H. We also thank Guangdong Provincial Science & Technology Project (2011B040300028) for financial support.

■ REFERENCES

(1) Barbe, V., Vallenet, D., Fonknechten, N., Kreimeyer, A., Oztas, S., Labarre, L., Cruveiller, S., Robert, C., Duprat, S., Wincker, P., Ornston, L. N., Weissenbach, J., Marliere, P., Cohen, G. N., and Medigue, C. (2004) Unique features revealed by the genome sequence of Acinetobacter sp ADP1, a versatile and naturally transformation competent bacterium. *Nucleic Acids Res. 32*, 5766–5779.

(2) Huang, W. E., Singer, A. C., Spiers, A. J., Preston, G. M., and Whiteley, A. S. (2008) Characterizing the regulation of the Pu promoter in Acinetobacter baylyi ADP1. *Environ. Microbiol. 10*, 1668–1680.

(3) Huang, W. E., Wang, H., Zheng, H. J., Huang, L. F., Singer, A. C., Thompson, I., and Whiteley, A. S. (2005) Chromosomally located gene fusions constructed in *Acinetobacter sp* ADP1 for the detection of salicylate. *Environ. Microbiol. 7*, 1339–1348.

(4) Perron, G. G., Lee, A. E. G., Wang, Y., Huang, W. E., and Barraclough, T. G. (2012) Bacterial recombination promotes the evolution of multi-drug-resistance in functionally diverse populations. *Proc. R. Soc. B 279*, 1477−1484.
(5) Zhang, D., He, Y., Wang, Y., Wang, H., Wu, L., Aries, E., and Huang, W. E. (2012) Whole-cell bacterial bioreporter for actively searching and sensing of alkanes and oil spills. *Microb. Biotechnol. 5*, 87−97.
(6) Song, Y. Z., Li, G. H., Thornton, S. F., Thompson, I. P., Banwart, S. A., Lerner, D. N., and Huang, W. E. (2009) Optimization of bacterial whole cell bioreporters for toxicity assay of environmental samples. *Environ. Sci. Technol. 43*, 7931−7938.
(7) Zhang, D. Y., Fakhrullin, R. F., Ozmen, M., Wang, H., Wang, J., Paunov, V. N., Li, G. H., and Huang, W. E. (2011) Functionalization of whole-cell bacterial reporters with magnetic nanoparticles. *Microb. Biotechnol. 4*, 89−97.
(8) Schell, M. A., and Ornston, L. N. (1993) Molecular biology of the LysR family of transcriptional regulators. *Annu. Rev. Microbiol. 47*, 597−626.
(9) Ezezika, O. C., Collier-Hyams, L. S., Dale, H. A., Burk, A. C., and Neidle, E. L. (2006) CatM regulation of the benABCDE operon: Functional divergence of two LysR-type paralogs in Acinetobacter baylyi ADP1. *Appl. Environ. Microbiol. 72*, 1749−1758.
(10) Jones, R. M., Pagmantidis, V., and Williams, P. A. (2000) sal genes determining the catabolism of salicylate esters are part of a supraoperonic cluster of catabolic genes in Acinetobacter sp strain ADP1. *J. Bacteriol. 182*, 2018−2025.
(11) Ruangprasert, A., Craven, S. H., Neidle, E. L., and Momany, C. (2010) Full-length structures of BenM and two variants reveal different oligomerization schemes for LysR-type transcriptional regulators. *J. Mol. Biol. 404*, 568−586.
(12) Bundy, B. M., Collier, L. S., Hoover, T. R., and Neidle, E. L. (2002) Synergistic transcriptional activation by one regulatory protein in response to two metabolites. *Proc. Natl. Acad. Sci. U.S.A. 99*, 7693−7698.
(13) Fischer, R., Bleichrodt, F. S., and Gerischer, U. C. (2008) Aromatic degradative pathways in *Acinetobacter baylyi* underlie carbon catabolite repression. *Microbiology 154*, 3095−3103.
(14) Romeroarroyo, C. E., Schell, M. A., Gaines, G. L., and Neidle, E. L. (1995) CatM encodes a LysR-Type transcriptional activator regualting catechol degradation in *Acinetobacter calcoaceticus*. *J. Bacteriol. 177*, 5891−5898.
(15) Collier, L. S., Gaines, G. L., and Neidle, E. L. (1998) Regulation of benzoate degradation in *Acinetobacter sp.* strain ADP1 by BenM, a LysR-Type transcriptional activator. *J. Bacteriol. 180*, 2493−2501.
(16) de Berardinis, V., Durot, M., Weissenbach, J., and Salanoubat, M. (2009) Acinetobacter baylyi ADP1 as a model for metabolic system biology. *Curr. Opin. Microbiol. 12*, 568−576.
(17) Wilkinson, D. J. (2009) Stochastic modelling for quantitative description of heterogeneous biological systems. *Nat. Rev. Genet. 10*, 122−133.
(18) Chu, D., Roobol, J., and Blomfield, I. C. (2008) A theoretical interpretation of the transient sialic acid toxicity of a *nanR* mutant of *Escherichia coli*. *J. Mol. Biol. 375*, 875−889.
(19) Kaern, M., Elston, T. C., Blake, W. J., and Collins, J. J. (2005) Stochasticity in gene expression: From theories to phenotypes. *Nat. Rev. Genet. 6*, 451−464.
(20) Pai, A., You, L. (2009) Optimal tuning of bacterial sensing potential, *Mol. Syst. Biol. 5*.
(21) Kennell, D., and Riezman, H. (1977) Transcription and translation initiation frequencies of *Escherichia-coli Lac* operon. *J. Mol. Biol. 114*, 1−21.
(22) Bauchop, T., and Elsden, S. R. (1960) The growth of micro-organisms in relation to their energy supply. *J. Gen. Microbiol. 23*, 457−469.
(23) Winson, M. K., Swift, S., Hill, P. J., Sims, C. M., Griesmayr, G., Bycroft, B. W., Williams, P., and Stewart, G. (1998) Engineering the luxCDABE genes from Photorhabdus luminescens to provide a bioluminescent reporter for constitutive and promoter probe plasmids and mini-Tn5 constructs. *FEMS Microbiol. Lett. 163*, 193−202.
(24) Juni, E., and Janik, A. (1968) Transformation of *Acinetobacter calcoaceticus* (Bacterium anitratum). *J. Bacteriol. 98*, 281−288.
(25) Delorenzo, V., Herrero, M., Jakubzik, U., and Timmis, K. N. (1990) MIini-Tn5 transposon derivatives for insertion mutagenesis, promoter probing, and chromosomal insertion of cloned DNA in Gram-negative eubacteria. *J. Bacteriol. 172*, 6568−6572.